

Formulation of Iron Oxide and Oxy-hydroxide Nanoparticles from Ilmenite Sand through a Low-Temperature Process

Tharindu P. B. Rajakaruna, Chandana P. Udawatte,* Rohana Chandrajith, and Rajapakse Mudiyansele Gamini Rajapakse



Cite This: *ACS Omega* 2021, 6, 17824–17830



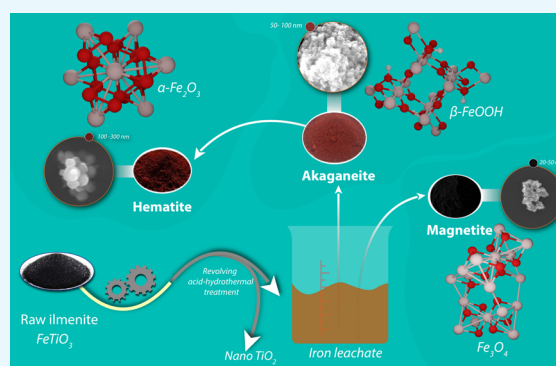
Read Online

ACCESS |

Metrics & More

Article Recommendations

ABSTRACT: In our previous publication, we published a simple, low-cost, and environmentally friendly process for the breaking down of the ilmenite lattice using rotary autoclaving, separation of titanium and iron components, and the conversion of the titanium component to amorphous TiO_2 and phase-specific titanium dioxide nanorods. Here, the separated iron component was converted into iron oxide (magnetite and hematite) and iron oxy-hydroxide (akaganeite, $\beta\text{-FeOOH}$) nanoparticles. The process flow diagram is presented to explain the steps involved. The materials synthesized are fully characterized by X-ray diffractogram (XRD), scanning electron microscopy coupled with energy-dispersive X-ray analysis (SEM-EDAX), and Fourier transform infrared (FT-IR), and it is shown that they contain 100% pure iron oxide and iron oxy-hydroxide nanoparticles without any detectable impurities. All of the chemical reactions involved in this process, which contribute to the mechanism of the process, are given. So far, such a low-cost, environmentally friendly, and low-temperature process has not been documented, and the process can be scaled-up for mass production of these nanomaterials used in various technological applications.



1. INTRODUCTION

Nanosized magnetic structures are currently key materials for advancements in electronics, optoelectronics, magnetic storage, and many bioinspired applications.^{1–4} The term ‘nanostructured systems’ comprises materials whose properties are determined by entities such as particles, crystallites, or clusters with characteristic lengths of between 1 and 100 nm, at least in two dimensions.⁵ If the grain or domain size becomes comparable or smaller to the characteristic length scale of the interaction processes controlling a particular property, different effects and unusual chemical and physical properties can be expected that are highly attractive in many technical applications.^{6–8} In recent years, large advancements have been achieved related to the synthesis and characterization of well-defined, discrete magnetic nanoparticles for both fundamental and technological purposes.^{9,10}

The polymorphic nature of iron is known for a long time. Iron nanoparticles (INPs) are among the most interesting novel materials due to their unique physicochemical properties such as high catalytic activity, high magnetism, low toxicity, and ability of microwave absorption.^{11–14} Iron nanoparticles can be classified into three major groups, namely¹⁵ (i) Iron oxide nanoparticles (IONs) (i.e., magnetite; Fe_3O_4 , hematite: $\alpha\text{-Fe}_2\text{O}_3$, maghemite; $\gamma\text{-Fe}_2\text{O}_3$), (ii) Iron oxy-hydroxide

(FeOOH) nanoparticles, and (iii) zero-valent iron (ZVI) nanoparticles.

These particles cover a wide range of applications including in drug delivery, magnetic targeting, hyperthermia, thermal-ablation, stem cell sorting and manipulation, gene therapy, negative magnetic resonance imaging (MRI) contrast enhancement, food preservation, bioprocess intensification, antimicrobial agents, bioseparation, ferrofluids, environmental remediation, lithium-ion batteries, and pigments.^{4,7–9,12,15}

Recently, the synthesis and characterization of magnetic nanoparticles have been attracted much attention due to the fact that they exhibit interesting magnetic properties that can be different from those of the bulk materials. Magnetite (Fe_3O_4), maghemite ($\gamma\text{-Fe}_2\text{O}_3$), and hematite ($\alpha\text{-Fe}_2\text{O}_3$) nanoparticles are mostly used as magnetic particles. These materials found to have extensive applications such as ferrofluids due to the high saturation magnetization (Ms),^{10–12} high magnetic susceptibility, and excellent bio-

Received: February 21, 2021

Accepted: June 21, 2021

Published: July 7, 2021



compatibility.^{6,12} However, magnetite (Fe_3O_4) nanoparticles are preferred magnetic particles in ferrofluids due to their greater saturation magnetization.¹²

The most favorable synthetic route for magnetite (Fe_3O_4) and hematite (Fe_2O_3) nanoparticles is the coprecipitation method because of its ease of use and higher yields compared to any other techniques.¹⁶ Coprecipitation from a solution of ferrous/ferric mixed salt has been widely used to produce magnetite nanoparticles due to its simplicity, capability of producing large volumes, and economic viability.¹⁴ Normal and reverse coprecipitations are the two known methods for adding precursors in the process of using a solution of ferrous/ferric mixed salt to synthesize magnetite. In the first method, the pH value gradually increases because an alkali solution is dropped into the mixed metal solution. In the second case, the mixed metal solution is directly dropped into an alkaline solution. Consequently, the pH, which is a critical factor in the synthesis of magnetite, could be easily controlled at high values.¹⁷

Similar to ferric oxide, anhydrous ferric oxy-hydroxide can be found in four different polymorph forms (akaganeite, goethite, lepidocrocite, and ferroxhyte). Among these, akaganeite ($\beta\text{-FeOOH}$) is known as the most preferred anhydrous form of FeOOH in chloride-containing environments. $\beta\text{-FeOOH}$ is widely used in waste water treatment and environmental remediation.¹⁸

Most previous studies on the synthesis of iron nanoparticles have used pure iron salts as the initial material,^{1–12} and no information was found on the formulation of iron products from natural ilmenite. In our previous work,¹⁹ a novel, low-cost, environmentally friendly method was introduced to prepare titanium dioxide nanoparticles from well-crystalline natural ilmenite (FeTiO_3). In that work, we reported the breaking down of the hard structure of ilmenite present in mineral sands using a rotary autoclave at low temperatures and mild acidic conditions. This has resulted in the separation of titanium fraction and leachate containing iron chloride. It described the methods for synthesizing phase-selective TiO_2 nanorods from the separated titanium fraction.

The novelty of this research is that it describes a novel, low-cost, significantly low-temperature process to break down the ilmenite structure and to separate the iron component and synthesize specific phases of iron oxide nanomaterials and zero-valent iron nanoparticles. In the present work, leachate containing iron chlorides was converted into magnetite, akaganeite, and hematite nanoparticles. The present study reports the procedure adapted to convert iron leachate to the above nanoparticles as by-products and their characterization.

2. RESULTS AND DISCUSSION

Figure 1a shows the powder X-ray diffractogram (P-XRD) of the black color powder obtained (product A) from coprecipitation path 1, as shown in Figure 5. The diffractogram peaks confirmed that product A is magnetite. The diffraction peaks that appear at 30.51, 35.82, 43.51, 53.83, 57.52, and 63.19° correspond to the (220), (311), (400), (422), (511), and (440) diffractions, respectively, of the pure magnetite phase of iron oxide (JCPDS Card No. 11-0614).⁶

Two brownish color powder products B and C were obtained from the coprecipitation path 2, and P-XRD patterns of those products are shown in Figures 1b,c, respectively. As shown in Figure 1b, diffraction peaks that appear at 26.72, 35.16, 39.24, 46.40, 56.88, and 61.46° correspond to the (310),

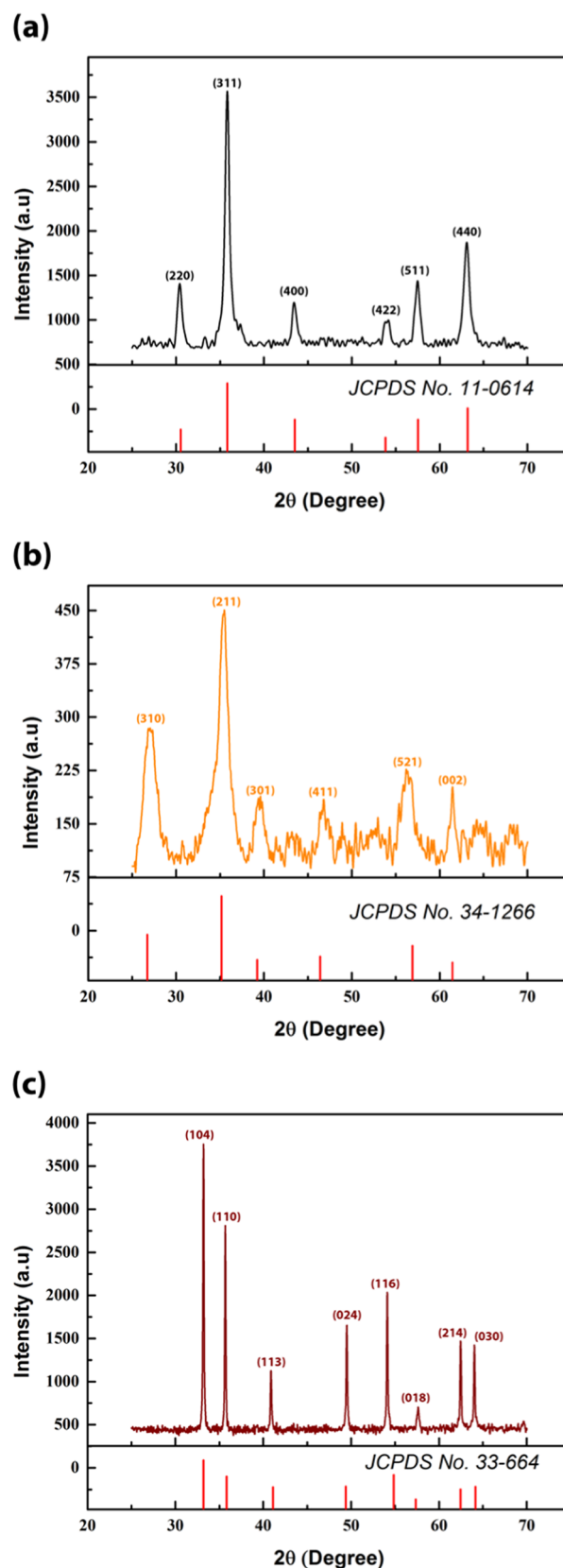


Figure 1. Powder X-ray diffraction patterns of (a) magnetite—product A, (b) akaganeite—product B, and (c) hematite—product C.

(211), (301), (411), (521), and (002) akaganeite phases of FeOOH , respectively (JCPDS Card No. 34-1266).¹⁸ Figure 1c shows the diffraction peaks that appear at 33.18, 35.82, 41.11,

49.38, 54.84, 57.35, 62.46, and 64.16° correspond to the (104), (110), (113), (024), (116), (018), (214), and (030) diffractions, respectively, of the hematite phase of iron oxide (JCPDS Card No. 33-664).²⁰

The crystallite diameters of prepared magnetite, akaganeite, and hematite calculated from the Debye–Scherrer equation using the FWHM of obtained XRD peaks (Figure 1) were 12, 06, and 54 nm, respectively.

The morphological studies of prepared products A, B, and C were carried out by scanning electron microscopy (SEM) observations (Figure 2). These images indicated that the prepared magnetite has a spherical morphology with around 20–50 nm in diameter. The SEM image of akaganeite, product

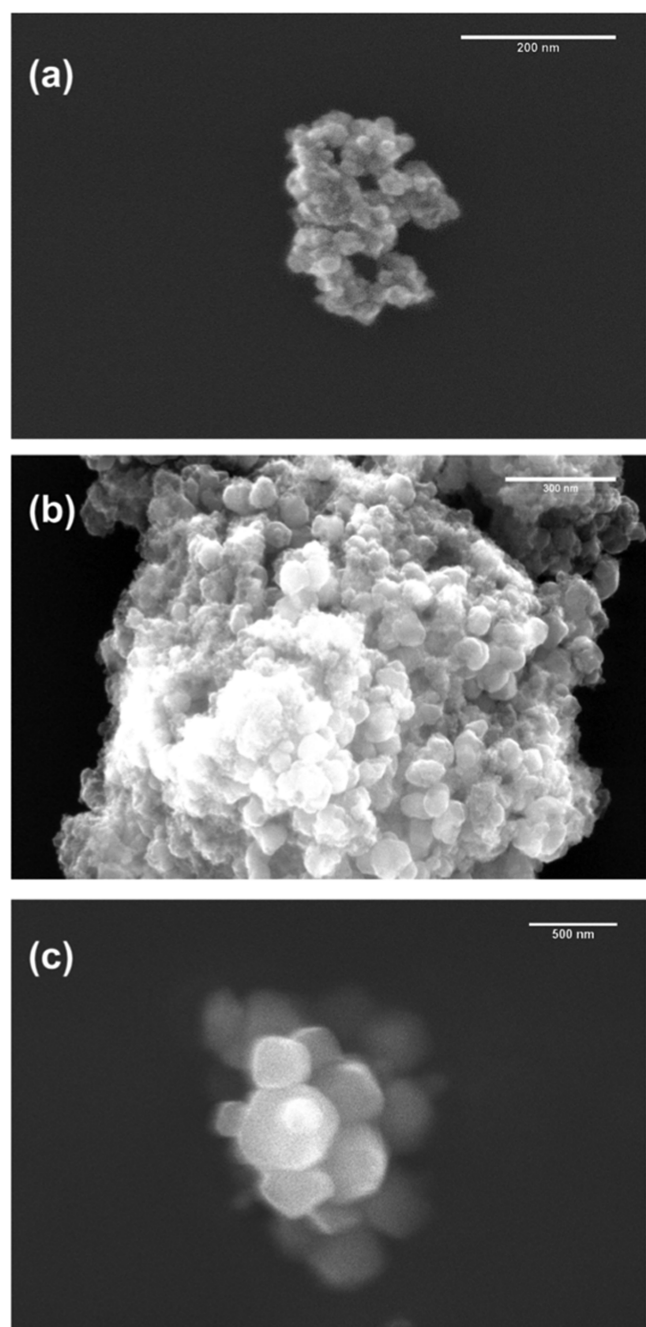


Figure 2. Scanning electron microscopic images of (a) magnetite—product A, (b) akaganeite—product B, and (c) hematite—product C.

B (Figure 2b), indicated spherical particle morphology with around 50–100 nm diameter. The SEM image of hematite, product C (Figure 2c), indicated a spherical shape morphology with particle size ranged approximately in 100–300 nm.

The SEM images give the morphology of particles. The sizes of the particles depend on the numbers of crystallite aggregated to form these particles. The different sizes in the same sample also show that even within the same material, different particles can have dissimilar numbers of aggregated crystallites. The fact that the akaganeite particle show larger sizes than magnetite particles in the SEM images show that more crystallites are arranged in the akaganeite particles than in magnetite particles.

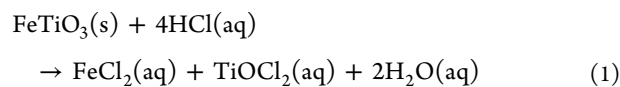
The purity of the as-prepared iron oxide and iron oxyhydroxide nanoparticles was confirmed by energy-dispersive X-ray (EDX) spectra. The results confirmed that products of magnetite, akaganeite, and hematite contain elements Fe and O only (Figure 3).

The EDS results show that the magnetite, akaganeite and hematite samples contain 100% Fe and O without any impurities.

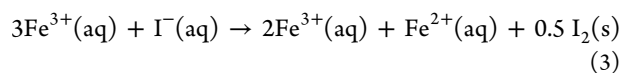
The X-ray detector hold in the EDS has been calibrated only for iron. However, the detector measures both Fe and O and calculates the atomic ratios based on the peak areas. The fact that the ratio shows more oxygen than the expected 1:1 ratio is possible due to contamination of oxygen during the sample preparation for the SEM analyses. It is also possible that oxygen molecules can be entrapped within the aggregates, leading to a higher oxygen percentage.

Figure 4a shows the FT-IR spectra of the prepared magnetite having peaks at wave number ranges 502–602, 621, 1500–1700, and 2800–3600 cm^{-1} , respectively for Fe–O stretching, Fe–O bending, O–H bending and O–H stretching vibration bands. FT-IR spectra of akaganeite showed vibration peaks of Fe–O at around 660 and 840 cm^{-1} , and broad peaks at 1500–1700 and 2800–3600 cm^{-1} that confirm the O–H bending and stretching vibrations (Figure 4b). The FT-IR spectra of the prepared hematite also showed (Figure 4c) peaks at wave number ranges 502–602, 621, 1500–1700 and 2800–3600 cm^{-1} , for Fe–O stretching, Fe–O bending, O–H bending and O–H stretching vibration bands, respectively.^{7,15}

In this study, initially, size-controlled ilmenite was leached with HCl in a revolving closed system (an autoclave), and the reaction that occurred in the autoclave is given in eq 1. The light green color $\text{FeCl}_2(\text{aq})$ solution oxidized to a more stable orange color $\text{Fe}^{3+}(\text{aq})$ solution with time.



The obtained iron(III) salt solution (reaction 2) from the acid hydrothermal process¹⁹ was mixed with a potassium iodide aqueous solution in a 3:1 mol ratio^{21,22} at room temperature, stirred, and allowed to reach the equilibrium within 1 h. The precipitate of iodine was filtered out (Whatman 40) and washed with distilled water, and the solution was also added to the filtrate.



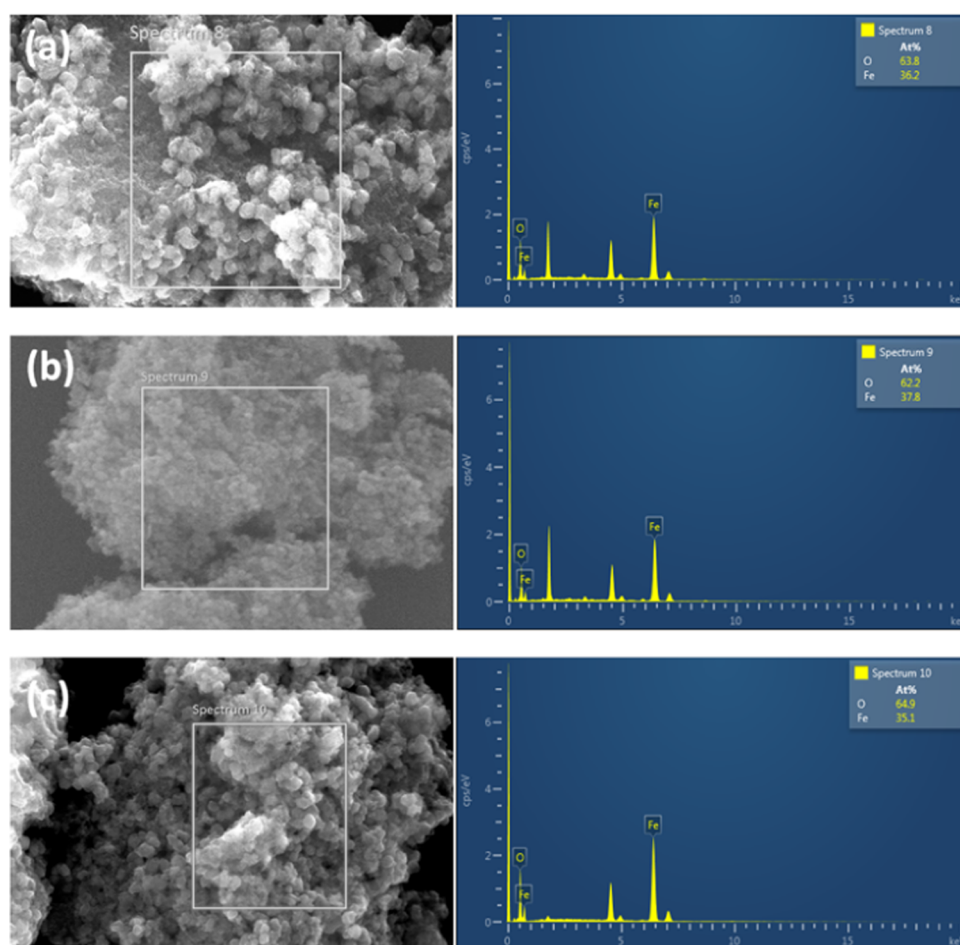
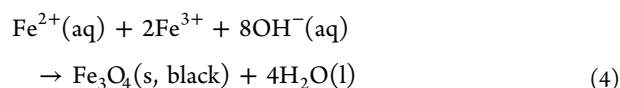
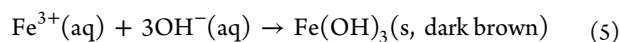


Figure 3. Energy-dispersive X-ray (EDX) spectrum of the (a) magnetite—product A, (b) akaganeite—product B, and (c) hematite—product C.

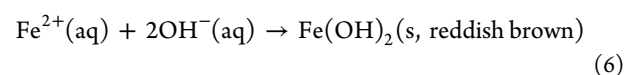
The iron salt solution that contained divalent (2+) and trivalent (3+) forms was initially acidic in nature. Generally, titration with a base solution triggered two important reactions.¹⁵ The first reaction occurred at the pH values of 2–4, while the second reaction occurred at the pH values of 8–9. A reddish-brown precipitate was observed during the first reaction, suggesting that Fe may be oxidized to intermediate ferric hydroxide [Fe(OH)₃]. However, the resultant brown precipitate turned into black color precipitate when the pH of the solution reached the second equivalent point (pH = 9), implying the formation of Fe₃O₄ nanoparticles by coprecipitation of Fe²⁺ and Fe³⁺ ions. The reaction stopped at the pH value of 12 to ensure that the precursors were fully reacted. Precipitation of divalent and trivalent Fe salts occurred in an alkaline medium, forming a black precipitate (Fe₂O₃ nanoparticle). The overall chemical reaction to synthesis Fe₃O₄ is given in eq 4.



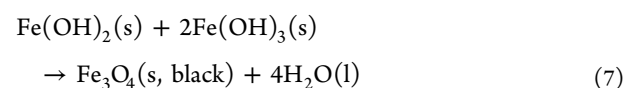
The trivalent Fe³⁺ solution was hydrolyzed and reacted to form the trivalent [Fe(OH)₃] intermediate compound at a pH value of between 2 and 4. According to a previous study,¹⁶ the reaction to form dark brown colored trivalent Fe(OH)₃ is proposed in the following reaction 5.



Then, the Fe²⁺ in the solution was reacted with the base to form reddish-brown precipitate of divalent ferrous hydroxide [Fe(OH)₂] at a pH value of between 7 and 9, given as reactions 6.



In this case, Fe(OH)₂ and Fe(OH)₃ salts were likely to be formed under a continuous titration reaction condition. From the titration curves, both salts reacted with each other at a pH of around 9 to form Fe₃O₄ nanoparticles. The chemical reaction is presented in reaction 7.



In the synthesis of akaganeite, initially, ilmenite was leached with HCl in a revolving closed system, and the reactions that occurred in the system are the same as reactions 1. Fe²⁺(aq) and FeCl₂(aq) thus with time obtained a light green color Fe²⁺(aq) solution that oxidized to a more stable orange color Fe³⁺(aq) solution, as mentioned in reaction 2. Iron salt solution was titrated with a base solution, and at a pH value of around 8–9, a reddish-brown precipitate was observed, suggesting that Fe may be oxidized to a ferric oxy-hydroxide [β-FeOOH] intermediate compound.²³ The proposed chemical reaction is given as follows

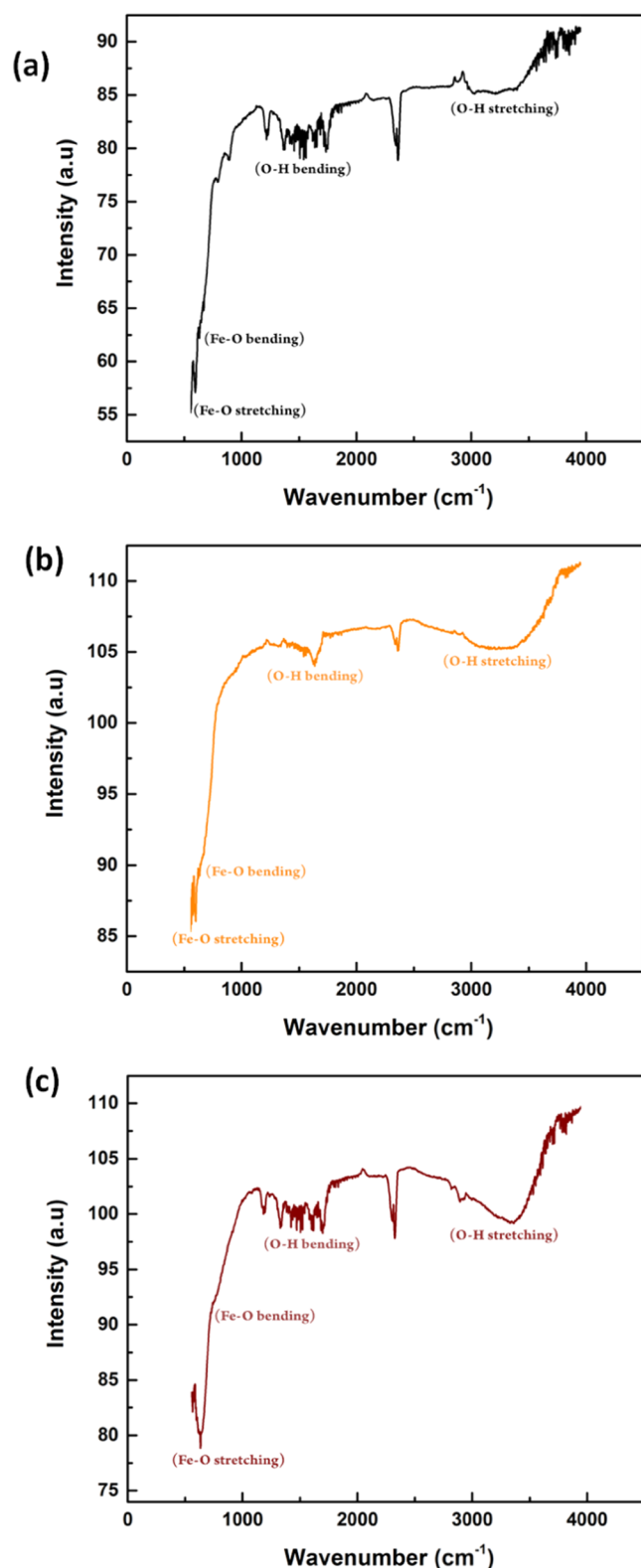
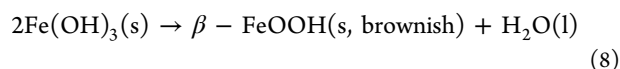
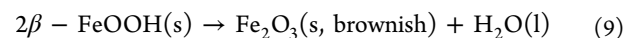


Figure 4. Fourier Transform Infrared Spectra of (a) magnetite—product A, (b) akaganeite—product B (c) hematite—product C.



During the calcination, the above intermediate akaganeite product converted into brownish hematite as described in chemical reaction 9.



This is the first time reporting of extraction of iron oxide nanoparticles from natural ilmenite, and the process warrants high feasibility for industrial scale as biproduction of TiO_2 from natural ilmenite.

3. CONCLUSIONS

A simple environmentally friendly process was developed to extract iron oxide (magnetite and hematite) and iron oxyhydroxide (akaganeite, $\beta\text{-FeOOH}$) nanoparticles from natural ilmenite sand. Characterization of the products obtained using various analytical techniques confirmed that they contain pure iron oxide nanoparticles. This study addressed the production of important by-products during the process of extraction of TiO_2 from ilmenite.

4. EXPERIMENTAL METHODS

Iron leachate was collected from the breakdown of natural ilmenite using an acid hydrothermal process according to our previous study.¹⁹

To obtain the magnetite from ilmenite, iron(III) solution leachate from an acid hydrothermal process was used as a precursor.¹⁹ The concentration of iron(III) in the leachate was determined by atomic absorption spectroscopy (Varian 240 FS). Based on the concentration of iron(III), the solution was mixed with a potassium iodide (Sigma-Aldrich) aqueous solution in a 3:1 mol ratio, and then mixed at room temperature, stirred, and allowed to reach the equilibrium by keeping 1 hour, allowing to obtain a complete precipitate. The precipitate of iodine was filtered and washed with distilled water. The filtrate was then hydrolyzed by adding 25% ammonia solution (Sigma-Aldrich) dropwise with continuous stirring until complete precipitation of the black magnetite obtained (at around pH 9 to 11). Finally, the set up was allowed to settle, then filtered and washed with distilled water, and dried at 80 °C overnight in a vacuum oven.

To obtain akaganeite, the resultant iron(III) solution leachate from the breakdown of ilmenite was directly hydrolyzed by adding 25% ammonia solution dropwise with continuous stirring until complete precipitation of the brown akaganeite was obtained (at around pH 7–9). Finally, the set up was allowed to settle, filtered, washed with distilled water, and dried at 80 °C overnight in a vacuum oven.

To produce hematite nanoparticles, the resultant akaganeite powder was calcined at 800 °C for 3 h.

The prepared iron oxide and oxyhydroxide nanoparticles were characterized by several analytical techniques. Material and phase identification was done by powder X-ray diffraction (Bruker D8 Advanced Eco X-ray Diffraction system) using copper-monochromatized $\text{Cu K}\alpha 1$ radiation under an acceleration voltage of 40 kV and a current of 40 mA. The morphology and dimensions of the particles of the products are revealed by their scanning electron microscopy (SEM) images using a JEOL JSM-6380 LA scanning electron microscope. Energy-dispersive X-ray analysis was performed to get the atomic percentages of the products. To study the functional groups of the synthesized products, the Fourier transform infrared spectra (FT-IR) were recorded using a Shimadzu FTIR-8400S, Prestige-21 spectrophotometer in a KBr matrix.

The process flowchart involving the entire process containing revolving autoclaving followed by coprecipitation

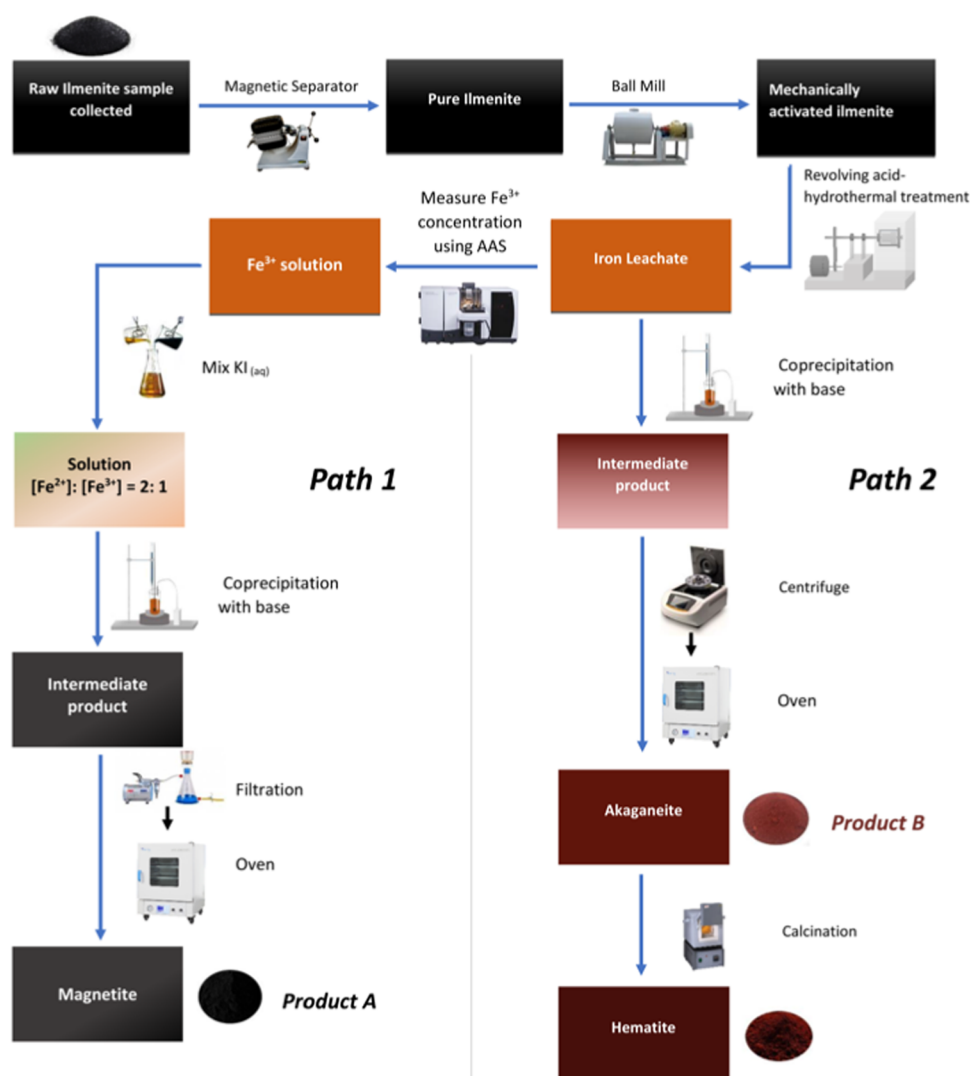


Figure 5. Process flow diagram for the conversion of raw ilmenite present in mineral sands to iron oxide nanomaterials.

to obtain pure iron oxide (magnetite and hematite) and oxyhydroxide (akaganeite) nanoparticles from natural ilmenite are shown in Figure 5.

AUTHOR INFORMATION

Corresponding Author

Chandana P. Udawatte – Department of Physical Sciences and Technology, Faculty of Applied Sciences, Sabaragamuwa University of Sri Lanka, 70140 Belihuloya, Sri Lanka; orcid.org/0000-0003-1723-7816; Email: chand@appsc.sab.ac.lk

Authors

Tharindu P. B. Rajakaruna – Faculty of Graduate Studies, Sabaragamuwa University of Sri Lanka, 70140 Belihuloya, Sri Lanka

Rohana Chandrajith – Department of Geology, Faculty of Science, University of Peradeniya, Peradeniya 20400, Sri Lanka

Rajapakse Mudiyansele Gamini Rajapakse – Department of Chemistry, Faculty of Science, University of Peradeniya, Peradeniya 20400, Sri Lanka; orcid.org/0000-0003-3943-5362

Complete contact information is available at: <https://pubs.acs.org/10.1021/acsomega.1c00938>

Author Contributions

All authors contributed equally to this manuscript.

Notes

The authors declare the following competing financial interest(s): Sri Lanka Patent No. SL/P/20883 with the same authors is under consideration.

ACKNOWLEDGMENTS

The authors thank E.M.S.B. Edirisuriya for assistance in obtaining SEM data, P.G.W. Ariyasena for assistance in obtaining XRD data, and M.B. Kularathna for assistance in drawing graphics. S.V. Bandara of “hNu” Studio-Sri Lanka is acknowledged for assistance in preparing the graphical abstract. The authors acknowledge the research funding provided by the Sabaragamuwa University of Sri Lanka under the research grant RG/2016/05.

■ REFERENCES

- (1) Daoush, W. M. Co-Precipitation and Magnetic Properties of Magnetite Nanoparticles for Potential Biomedical Applications. *Nanomed. Res. J.* **2017**, *5*, 3–8.
- (2) Prem Ananth, K.; Jose, S. P.; Venkatesh, K. S.; Ilangovan, R. Size controlled synthesis of magnetite nanoparticles using microwave irradiation method. *J. Nano Res.* **2013**, *24*, 184–193.
- (3) Daoush, W. M. Co-Precipitation and Magnetic Properties of Magnetite Nanoparticles for Potential Biomedical Applications. *J. Nanomed. Res.* **2017**, *5*, 3–8.
- (4) Ahn, T.; Kim, J. H.; Yang, H.; Lee, J. W.; Kim, J. Formation Pathways of Magnetite Nanoparticles by Coprecipitation Method. *J. Phys. Chem. C* **2012**, *116*, 6069–6076.
- (5) Khalaf, M. M.; Ibrahimov1, H. G.; Ismailov1, E. H. Nanostructured Materials: Importance, Synthesis and Characterization-A Review. *Chem. J.* **2012**, *2*, 118–125.
- (6) Goya, G. F.; Berquo, T. S.; Fonseca, F. C.; Morales, M. P. Static and dynamic magnetic properties of spherical magnetite nanoparticles. *J. Appl. Phys.* **2003**, *94*, 3520–3527.
- (7) Scherer, C.; Neto, A. M. F. Ferrofluids: Properties and Applications. *Braz. J. Phys.* **2005**, *35*, 718–726.
- (8) Ebrahiminezhad, A.; Hoseinabadi, A. Z.; Sarmah, A. K.; Taghizadeh, S.; Ghasemi, Y.; Berenjian, A. Plant-Mediated Synthesis and Applications of Iron Nanoparticles. *Mol. Biotechnol.* **2018**, *60*, 154–168.
- (9) Mamani, J. B.; Gamarra, L. F.; Brito, G. E. S. Synthesis and Characterization of Fe₃O₄ Nanoparticles with Perspectives in Biomedical Applications. *Mater. Res.* **2014**, *17*, 542–549.
- (10) Ali, A.; Zafar, H.; Zia, M.; Haq, I.; Phull, A. R.; Ali, J. S.; Hussain, A. Synthesis, characterization, applications, and challenges of iron oxide nanoparticles. *Nanotechnol., Sci. Appl.* **2016**, *9*, 49–67.
- (11) Issa, B.; Obaidat, I. M.; Albiss, B. A.; Haik, Y. Magnetic Nanoparticles: Surface Effects and Properties Related to Biomedicine Applications. *Int. J. Mol. Sci.* **2013**, *14*, 21266–21305.
- (12) Bartolome, L.; Imran, M.; Lee, K. G.; Sangalang, A.; Ahnd, J. K.; Kim, D. H. Superparamagnetic γ -Fe₂O₃ nanoparticles as an easily recoverable catalyst for the chemical recycling of PET. *Green Chem.* **2014**, *16*, 279–286.
- (13) Reinen, D. The Correlation between Structure and Color of Iron Oxide-type Solids, Sustainable Pigments with Gentle Hues. *Z. Anorg. Allg. Chem.* **2014**, *640*, 2677–2683.
- (14) Liu, J.; Cheng, J.; Che, R.; Xu, J.; Liu, M.; Liu, Z. Synthesis and Microwave Absorption Properties of Yolk–Shell Microspheres with Magnetic Iron Oxide Cores and Hierarchical Copper Silicate Shells. *ACS Appl. Mater. Interfaces* **2013**, *5*, 2503–2509.
- (15) Ealia, S. A. M.; Saravanakumar, M. P. A review on the classification, characterization, synthesis of nanoparticles and their application. *IOP Conf. Ser.: Mater. Sci. Eng.* **2017**, *263*, No. 032019.
- (16) Mutasim, K. Co-precipitation in aqueous solution synthesis of magnetite nanoparticles using iron (III) salts as precursors. *Arabian J. Chem.* **2015**, *8*, 279–284.
- (17) Baalousha, M. Aggregation and disaggregation of iron oxide nanoparticles: Influence of particle concentration, pH and natural organic matter. *Sci. Total Environ.* **2009**, *407*, 2093–2101.
- (18) Chen, M.; Jiang, J.; Zhou, X.; Diao, G. Preparation of Akaganeite Nanorods and Their Transformation to Sphere Shape Hematite. *J. Nanosci. Nanotechnol.* **2008**, *8*, 3942–3948.
- (19) Rajakaruna, T. P. B.; Udawatte, C. P.; Chandrajith, R.; Rajapakse, R. M. G. Nonhazardous Process for Extracting Pure Titanium Dioxide Nanorods from Geogenic Ilmenite. *ACS Omega* **2020**, *5*, 16176–16182.
- (20) Red'ko, Y. V.; Suprun, N. P. XRD and SEM analysis of iron oxide nanoparticles formation in polyamide textile material. *Fibres Text* **2018**, *3*, 63–67.
- (21) Jiang, W.; Lai, K. L.; Hu, H.; Zeng, X. B.; Lan, F.; Liu, K. X.; Yao Wu, Y.; Gu, Z. W. The effect of [Fe³⁺]/[Fe²⁺] molar ratio and iron salts concentration on the properties of superparamagnetic iron oxide nanoparticles in the water/ethanol/toluene system. *J. Nanopart. Res.* **2011**, *13*, 5135–5145.
- (22) Alibeigi, S.; Vaezi, M. R. Phase Transformation of Iron Oxide Nanoparticles by Varying the Molar Ratio of Fe²⁺: Fe³⁺. *Chem. Eng. Technol.* **2008**, *31*, 1591–1596.
- (23) Basavegowda, N.; Mishra, K.; Lee, Y. R. Synthesis, characterization, and catalytic applications of hematite (α -Fe₂O₃) nanoparticles as reusable nanocatalyst. *Adv. Nat. Sci.: Nanosci. Nanotechnol.* **2017**, *8*, No. 025017.